APPLIED GEOPHYSICS, Vol.14, No.2 (June 2017), P. 236–246, 9 Figures.
DOI:10.1007/s11770-017-0616-y

Improving the resolution of seismic traces based on the secondary time–frequency spectrum*

Wang De-Ying♦[1,2,3], Huang Jian-Ping[1], Kong Xue[4], Li Zhen-Chun[1], and Wang Jiao[1]

Abstract: The resolution of seismic data is critical to seismic data processing and the subsequent interpretation of fine structures. In conventional resolution improvement methods, the seismic data is assumed stationary and the noise level not changes with space, whereas the actual situation does not satisfy this assumption, so that results after resolution improvement processing is not up to the expected effect. To solve these problems, we propose a seismic resolution improvement method based on the secondary time–frequency spectrum. First, we propose the secondary time-frequency spectrum based on S transform (ST) and discuss the reflection coefficient sequence and time-dependent wavelet in the secondary time–frequency spectrum. Second, using the secondary time–frequency spectrum, we design a two-dimensional filter to extract the amplitude spectrum of the time-dependent wavelet. Then, we discuss the improvement of the resolution operator in noisy environments and propose a novel approach for determining the broad frequency range of the resolution operator in the time–frequency–space domain. Finally, we apply the proposed method to synthetic and real data and compare the results of the traditional spectrum-modeling deconvolution and Q compensation method. The results suggest that the proposed method does not need to estimate the Q value and the resolution is not limited by the bandwidth of the source. Thus, the resolution of the seismic data is improved sufficiently based on the signal-to-noise ratio (SNR).
Keywords: resolution, S transform, time–frequency spectrum, time-variant wavelet, spectrum-modeling deconvolution, Q compensation

Introduction

Enhancing the resolution of seismic data is critical to seismic data processing. Consequently, a plethora of methods has been proposed to enhance seismic data resolution, e.g., deconvolution, spectral whitening, impedance-constrained inversion, etc. These methods are mostly based on the stationary convolution model, in which the wavelet is time-invariant. The actual seismic

Manuscript received by the Editor February 26, 2017; revised manuscript received May 13, 2017.
*This research was financially supported by the National 973 Project (No. 2014CB239006), the National Natural Science Foundation of China (No. 41104069 and 41274124) and the Fundamental Research Funds for Central Universities (No. R1401005A).
1. College of Geosciences, China University of Petroleum, Qingdao 266580, China.
2. Post-Doctoral Scientific Research Station, BGP, CNPC, Zhuozhou 072751, China.
3. College of Earth Science and Engineering, Shandong University of Science and Technology, Qingdao 266590, China.
4. College of Petroleum Engineering Shengli College China University of Petroleum, Dongying 257061, China.
♦Corresponding author: Wang De-Ying (Email: wangdede@126.com)

records do not satisfy the requirements of the stationary convolution model and do not yield satisfactory results.

With the development of time-frequency analysis techniques, many absorption compensation and deconvolution methods based on non-stationary signals can be used to compensate for energy loss caused by formation transmission and absorption and carry out compression of wavelets to improve resolution of seismic data.

Bai and Li (1999) used the short-time Fourier transform to obtain the absorption factor at each time and frequency based on the stratigraphic absorption characteristics and then used the weighted short-time Fourier transform coefficient to reconstruct the reflection seismogram and to eliminate the stratigraphic absorption. This method can be used to compensate the absorbed energy without estimating the Q values in advance and can be applied to depth-variable Q values. To improve the precision of the absorption-compensation method, Liu et al. (2006) used the generalized S transform. The stratigraphic absorption of the seismic wave energy attenuates the amplitude and changes the wavelet phase. Zhou et al. (2014) proposed a method for compensating the amplitude and phase spectra based on the generalized S transform. Their method can recover the amplitude spectrum of the strata reflections, while eliminating the effect of the residual phase of the wavelet. Thus, the wavelet approaches the zero-phase wavelet and the seismic resolution is improved. To remove most of the effects resulting from the wavelet truncation and interference, which are common in the time–frequency absorption-compensation method, Wang et al. (2010) proposed a new formation absorption-compensation method based on adaptive molecular decomposition to realize stratigraphic absorption compensation for seismic records of heterogeneous viscoelastic media with thin layers.

To make the deconvolution methods suitable for nonstationary signal processing, Margrave et al. (2001) and Margrave et al. (2011) proposed a nonstationary convolution model for deconvolution in the Gabor domain. Ahadi and Riahi (2013) designed the Gabor deconvolution operator using the downgoing wavefield of zero-offset VSP data and applied it to the upgoing wavefield. Chen et al. (2013) used the regularized smoothing method to determine the Gabor deconvolution operator and applied it to nonstationary seismic data. Sun et al. (2014) used Gabor deconvolution to handle nonstationary and sparsity-constrained deconvolution to separate reflectivity and wavelet. The conventional nonstationary convolutional model assumes that the seismic signal is recorded at normal incidence; however, raw shot gathers cannot be treated in this manner because of offsets. Thus, Li (2013) proposed a prestack nonstationary deconvolution method based on variable-step sampling in the radial trace domain.

The abovementioned methods perform well because they consider the time-variant characteristics of the seismic wavelet but neglect the absorption owing to oil and gas (Goloshubin and Bakulin, 1998; Goloshubin and Korneev, 2000; Castagna et al., 2003; Xue et al., 2013). After enhancing the resolution of seismic data, the characteristics of local energy anomalies may be destroyed, affecting the quality of processing results that largely depend on the separation of the time-variant wavelet and the reflection coefficient sequence.

Compared with the wavelet transform and the Curvelet and Shearlet transforms, the short-time Fourier transform, and the Gabor and S transforms provide instantaneous information on the signal with time and maintain the spectrum characteristics of the Fourier transform. Hence, we can easy extend the improvement resolution methods from frequency domain to these time-frequency domain. Compared with the short-time Fourier transform and Gabor transform, the frequency in the S transform is inversely proportional to the Gauss windows width, satisfying the demand for high-resolution and high-frequency components in energy compensation processing (Stockwell et al., 1996; Djeffal, 2016). Below, we proceed in enhancing the resolution in the ST domain.

Compared with the frequency spectrum characteristic of the reflection coefficient sequence, it is well known that the seismic wavelet energy gradually attenuates with time and the bandwidth slowly narrows; that is, the energy of the seismic wavelet slowly changes with time. The time–frequency spectrum of the S transform describes the amplitude change at different frequencies and local time, and shows the amplitude distribution of the time–frequency plane. The amplitude of the local time–frequency cell is thus obtained but not the rate of the amplitude change with time and frequency. Obviously, it is difficult to obtain the amplitude spectrum of the time-varying wavelet in the S domain.

To solve the problem of obtaining the information that describes the amplitude spectrum change with time and frequency in the S domain, combining the conclusions obtained by Ricker's (1977) research work, and inspired by the work of Rosa et al. (1991) and Tang (2010) et al., we consider the time–frequency spectrum of the seismic data real and perform two-dimensional Fourier transform (2D FT) to obtain the second-order spectrum

of the seismic data, which we call the secondary time–frequency spectrum. We analyze the characteristics of the amplitude spectrum of the time-variant wavelet and the reflection coefficient sequence in the secondary time-frequency spectrum plane of the seismic data. Then, we use a 2D filter to separate the amplitude spectrum of the time-variant wavelet and the reflection coefficient sequence. The spectrum anomalies owing to oil or gas in the strata are thus avoided and the proposed method preserves the amplitude. In designing the operator for enhancing the resolution, we consider the spatial variation of SNR; thus, this method has the ability to adapt to the time and space variations of the seismic data.

Amplitude spectrum extraction of time-variant wavelet

Secondary time–frequency spectrum

The scattering of the seismic wave energy and absorption by the strata make the frequency of the seismic data time-variant. To process such seismic data, we typically use the wavelet transform, Curvelet transform, Shearlet transform, Gabor transform, and S transform. There is inverse proportion relation between the Gauss window width of the S transform; When high frequency compensation is satisfied, high frequency components have high resolution (Djeffal, 2016). Therefore, we improves the resolution processing in the S transform domain. The ST of signal $x(t)$ is defined as (Stockwell et al., 1996)

$$S(\tau, f) = \int_{-\infty}^{\infty} x(t) w(\tau - t, f) e^{-i2\pi ft} dt. \quad (1)$$

The Gauss window function $w(\tau - t, f)$ is expressed as

$$w(\tau - t, f) = \frac{|f|}{\sqrt{2\pi}} e^{\frac{-f^2(\tau - t)^2}{2}}. \quad (2)$$

The inverse S transform (IST) is

$$x(t) = \int_{-\infty}^{\infty} S(\tau, f) e^{i2\pi ft} df. \quad (3)$$

$A(\tau, f)$ is the amplitude spectrum of the time–frequency of $x(t)$

$$A(\tau, f) = |S(\tau, f)|, \quad (4)$$

where || denote absolute values. The amplitude spectrum of the S transform describes the variation of amplitude at different frequencies with time, which gives the amplitude distribution in the time–frequency plane. Owing to the scattering and strata absorption, the amplitude spectrum of the time-variant wavelet is slowly changing with time. The logging data suggest that the amplitude of the reflection coefficient sequence changes fast at different frequencies (Painter, et al., 1995). Obviously, the amplitude distribution in the time –frequency domain produced by the S transform cannot describe the rate of amplitude change with time and frequency.

By applying the Fourier transform, we transform the signal information into the frequency domain to describe the rate of amplitude change with time. To obtain the amplitude change with time and frequency, we treat the amplitude of the time–frequency spectrum of the S transform as signal and apply the Fourier transform to it.

We apply the one-dimensional Fourier transform to $A(\tau, f)$ in the time domain and the result is expressed as

$$A^{(2)}(w, f) = \int_{-\infty}^{\infty} A(\tau, f) e^{-i2\pi w\tau} d\tau, \quad (5)$$

where w corresponds to τ and represents the frequency, and $A^{(2)}(w, f)$ describes the amplitude of the local frequency change with time.

We then apply one-dimensional Fourier transform to $A^{(2)}(w, f)$ in the frequency domain and express $A^{(2)}(w, f^{(2)})$, where $f^{(2)}$ corresponds with f, as

$$A^{(2)}(w, f^{(2)}) = \int_{-\infty}^{\infty}\int_{-\infty}^{\infty} A(\tau, f) e^{-i2\pi w\tau} e^{-i2\pi ff^{(2)}} d\tau df. \quad (6)$$

In fact, the information in the frequency domain returns to the time domain after the Fourier transform; thus, $f^{(2)}$ represents the time and the result describes the amplitude of the local time change with frequency.

By applying the 2D FT to the time–frequency amplitude spectrum $A(\tau, f)$, we obtain the parameter that describes the amplitude spectrum change as a function of local time and frequency, and we call it the secondary

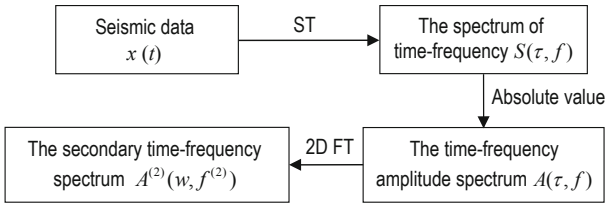

Fig.1 Flowchart for obtaining the secondary time–frequency spectrum from seismic data.

time–frequency spectrum. Figure 1 shows the flowchart for obtaining the secondary time–frequency spectrum from seismic data.

Amplitude spectrum of the time-variant wavelet

The amplitude spectrum of wavelet generally relatively smooth, whereas the reflection coefficient is rougher. In the S domain, the amplitude spectrum at local time is oscillating and the sharp oscillations are attributed to the reflection coefficient, whereas the slowly changing parts are attributed to the time-variant wavelet. After transforming seismic data to the secondary time –frequency spectrum, the energy of the time-variant wavelet components are mainly located in the low-frequency spectrum along the $f^{(2)}$ axis and the reflection coefficient components are mainly concentrated in the high-frequency spectrum along the $f^{(2)}$ axis. We then use a low-pass filter to extract the instantaneous wavelet along $f^{(2)}$.

As seismic waves propagate underground, spherical diffusion and the viscosity of layers filled with fluid(s) cause the wavelet energy to attenuate with time. The attenuation caused by oil-bearing layers in local time is used in reservoir prediction (Che-Alota, et al., 2008; Quintal, et al., 2008; Wang, et al., 2014). The amplitude spectrum of time-variant wavelet, which is used to enhance the resolution operator, should eliminate the attenuation anomalies and enhances the seismic resolution. The absorption anomalies in the amplitude spectrum of the instantaneous wavelet owing to oil-bearing layers along the time direction oscillate in local time. We thus use the oscillating curve as the real signal and apply FFT to it. The absorption anomalies are concentrated in the high-frequency region along the w-axis in the secondary time–frequency spectrum. Assuming the attenuation owing to spherical diffusion and strata absorption changes slowly and the response of the reflection coefficient and anomalies owing to oil-bearing layers change markedly with time, a low-pass filter is designed to extract the amplitude spectrum of time-variant along the w-axis in the secondary time–frequency spectrum.

In summary, in the secondary time–frequency spectrum, the components of the time-variant wavelet are at the center, whereas the low-amplitude components of the reflection coefficients are adjacent. We use a two-dimensional low-pass filter (2D LPF) to extract the amplitude spectrum of time-variant wavelet. The 2D LPF operator is

$$H(w, f^{(2)}) = H_1(w)H_2(f^{(2)}), \tag{7}$$

where $H_1(w)$ and $H_2(f^{(2)})$ are one-dimensional filters. The attenuation of the time-variant wavelet along the w- and $f^{(2)}$-direction differs; therefore, $H_1(w)$ and $H_2(f^{(2)})$ are respectively defined as

$$H_1(w) = e^{kw^2}, \text{ where } k < 0, \tag{8}$$

$$H_2(f^{(2)}) = \begin{cases} \text{when } \left|f^{(2)}\right| < f_{h2}, \text{where } f_{h2} \text{ is} \\ \text{the maximum value } f^{(2)} \text{ which} \\ 1, \text{ satisfy the condition of} \\ |A^{(2)}(w, f^{(2)})| > \delta \max\{|A^{(2)}(w, f^{(2)})|\}; \\ \delta \text{ is a small constant.} \\ 0, \text{ orthers}. \end{cases} \tag{9}$$

To further show the differences between the time-variant wavelet and reflection coefficient in the secondary time–frequency spectrum, we use a synthetic nonstationary seismic record (Figure 2) and compare it to the time-variant wavelet in the secondary time–frequency spectrum. The synthetic stationary seismic record (Figure 2b) is the result of the convolution of a 30 Hz Ricker and the reflection coefficient sequence (Figure 2a) after Q filtering (Figure 2c). We calculate the secondary time–frequency spectrum of the time-variant wavelet and that of the synthetic nonstationary record, and show the results in Figure 3. The secondary time–frequency spectrum of the time-variant wavelet (Figure 3a) and the central area of the secondary time–frequency spectrum of the nonstationary seismic data are similar (Figure 3b), whereas the reflection coefficient sequence is far from the center. Thus, the time-variant wavelet and the reflection coefficient sequence have different

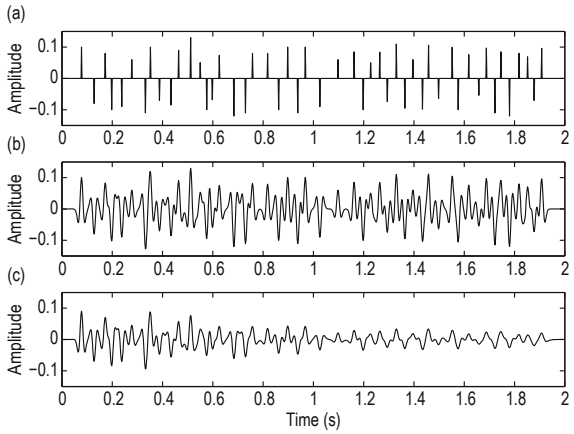

Fig.2 Synthetic nonstationary seismic record: (a) reflection coefficient sequence; (b) Synthetic stationary seismic record; (c) Synthetic nonstationary seismic record: the result of Fig. 2b after Q filtering.

Secondary time–frequency spectrum

secondary time–frequency spectra. The processing of the time-variant wavelet spectrum has the following steps.

(1) Use equation (6) to transform the nonstationary seismic data $x(t)$ to the secondary time–frequency spectrum $A^{(2)}(w, f^{(2)})$.

(2) Design the 2D LPF $H(w, f^{(2)})$ for the secondary time–frequency spectrum plane.

(3) Multiply $A^{(2)}(w, f^{(2)})$ and $H(w, f^{(2)})$, and then perform 2D IFT to obtain the amplitude spectrum of the time-variant wavelet and denote it as $W(\tau, f)$.

Note that the extraction of the time-variant wavelet amplitude spectrum is from one trace to another, owing to the difference of amplitude and frequency among the traces, and thus the lateral continuity after enhancing the seismic resolution may deteriorate. To overcome this problem, we use weighted processing.

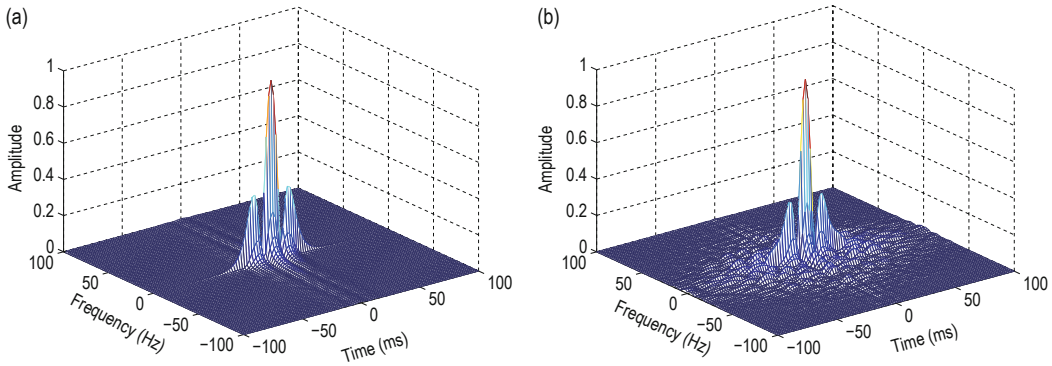

Fig.3 Comparison the secondary time–frequency amplitude spectrum of the time-variant wavelet (a) and that of synthetic nonstationary seismic record (b) (amplitude after normalization).

Enhancing resolution operator

In noisy environments, the operator is critical to the SNR and resolution enhancement. Berkhout (1977) derived by using least squares the inverse filtering operator in the frequency domain, with optimum trade-off between noise amplification and recovery of reflectivity. The inverse filtering operator is

$$P(f)=\frac{W(f)}{|W(f)|^2+\sigma^2}, \tag{10}$$

where $W(f)$ denotes the amplitude spectrum of the seismic wavelet and σ^2 denotes the noise variance. Subsequently, van der Baan (2008) designed the time-varying inverse filtering operator for time-varying deconvolution. Margrave et al. (2011) designed the following time-varying amplitude compensation operator

$$P(t,f)=\frac{W_{\max}}{W(t,f)+\varepsilon W_{\max}}, \tag{11}$$

where ε is a small positive constant, as the standard prewhitening constant in Robinson deconvolution, and $W_{\max}$ is

$$W_{\max}=\max\{W(t,f)\}. \tag{12}$$

As the actual seismic records are affected by the acquisition environment, the noise level varies spatially, so the estimation of noise levels is also accompanied by errors. It is obvious that the single noise level parameter will not adapt to the change of signal to noise ratio in the whole exploration area, and reduces the adaptation of the inverse operator. The relative strength between the frequencies in amplitude spectrum of a post seismic record at a given time and location shows the S/N value in the frequency range at a certain extent. To adapt the spatial variation of SNR, we design the following inverse filtering operator

$$P(t,f)=\begin{cases}1, & f<f_a \text{ or } f>f_d\\ \dfrac{W_{\max}}{W(t,f)+\varepsilon W_{\max}}, & f_b<f<f_c\\ 1-\lambda+\dfrac{\lambda W_{\max}}{W(t,f)+\varepsilon W_{\max}}, & f_a\le f\le f_b \text{ or } f_c\le f\le f_d\end{cases}, \tag{13}$$

where λ $(0\le\lambda\le 1)$ is the weighting factor for the slope and decreases with increasing distance from the

dominant frequency, f_a, f_b, f_c, and f_d are bandwidth control parameters and satisfy the condition $f_a<f_b<f_c<f_d$ based on the following equation

$$\begin{cases} \dfrac{W(t_x, f_a)}{\max\{W(t_x, f)\}} = a, \\ \dfrac{W(t_x, f_b)}{\max\{W(t_x, f)\}} = b, \\ \dfrac{W(t_x, f_c)}{\max\{W(t_x, f)\}} = c, \\ \dfrac{W(t_x, f_d)}{\max\{W(t_x, f)\}} = d, \end{cases}, \tag{14}$$

where $t_x \in t$, and a, b, c, and d are constants that control the extent of band broadening and satisfy $0< a$, b, c, $d<1$ and $b>a$, $c>d$; the smaller the values, the stronger the degree of band broadening. In real seismic data processing, the selection of parameter values is based on the SNR and the wavelet bandwidth. The latter varies as a function of time and space; therefore, the degree of bandwidth expansion also changes as a function of time and space. The flowchart for improving the seismic resolution based on the secondary time–frequency spectrum is shown in Figure 4.

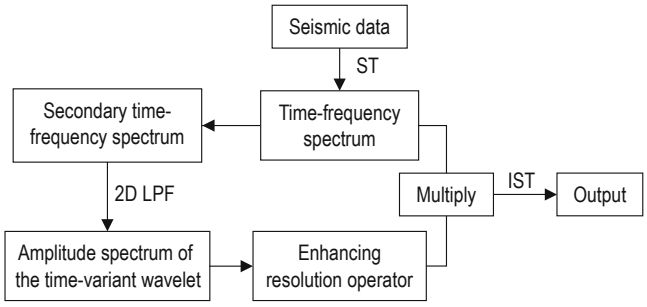

Fig.4 Flowchart of the seismic resolution improvement based on the secondary time–frequency spectrum.

Model testing

To test the proposed method, model and real seismic data are processed, based on conventional spectrum modeling deconvolution and Q compensation.

Synthetic stationary seismic records are obtained by convoluting a 30 Hz Ricker wavelet using the reflection coefficient sequence (Figure 5a). Then, we obtain the synthetic nonstationary seismic record (Figure 5b) following Q filtering. The energy of the seismic data decreases gradually with time. We use traditional spectrum-modeling deconvolution, the Q compensation method, and the proposed method to improve the resolution of the synthetic nonstationary seismic record and show the results in Figure 5.

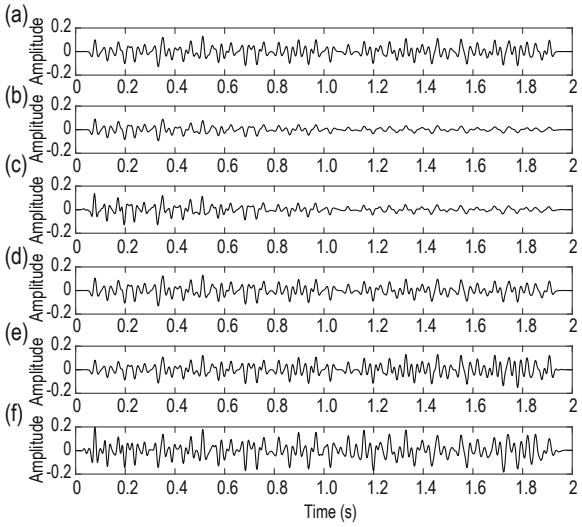

Fig.5 Model test: (a) synthetic stationary seismic record; (b) synthetic nonstationary seismic record obtained from Fig. 5a after Q filtering; (c) results of Fig. 5b after spectrum modeling deconvolution; (d) results of Fig. 5b after Qcompensation with +20% Q estimation error; (e) results of Fig. 5b after Q compensation with -20% Q estimation error; (f) results of Fig. 5b using the proposed processing method.

The comparison of the waveforms before and after spectrum-modeling deconvolution (Figures 5b and 5c) shows that the waveform is compressed and the resolution is improved between 0.0 s and 0.6 s, whereas the amplitude and waveform do not change significantly after processing and the resolution does not improve between 1.0 s and 2.0 s. Traditional spectrum-modeling deconvolution assumes that seismic data are stationary and the seismic wavelet is nonvariant. When processing nonstationary seismic signals, traditional spectrum-modeling deconvolution does not consider local time–frequency variations; therefore, the results are unsatisfactory.

In processing with the proposed method in the time –frequency domain, the resolution operator is time-dependent and adaptable to nonstationary seismic data. The comparison of the resolution results before (Figure 5b) and after (Figure 5f) processing with the proposed method shows that the resolution has improved and the influence of attenuation is minimized because the attenuation energy of the wavelet is compensated and the amplitude relation between each reflection signal is

restored.

To further compare and analyze the proposed method, we perform Q compensation on synthetic nonstationary seismic data (Figure 5b) with +20%, 0%, and −20% Q estimation error and compare the results with those of the proposed method. Figures 5d and 5e show the results of the Q compensation with +20% and −20% Q estimation error, respectively. The Q compensation results are the same with the data before the Q attenuation (Figure 5a). The comparison of Figures 5d, 5a, 5e, and 5f shows that the Q compensation results are unsatisfactory when Q estimation error is existence and that the Q compensation method eliminates the time-variability of the wavelet and restores the propagating wavelet to the level of the source wavelet under the condition of accurate Q values, without considering spherical diffusion and scattering. Based on the results of the proposed method, it can be seen that the resolution of shallow, medium, and deep layers has improved, whereas the resolution of the wavelet of shallow and middle layers is much larger than that of the Ricker wavelet. The latter suggests that the proposed method can improve the resolution while compensating for the absorption of the formation; the results are better than that of the Q compensation method in shallow and middle layers.

To analyze the bandwidth changes before and after processing, we calculate and compare the time–frequency spectrum, as shown in Figure 6. Figure 6a shows the time–frequency spectrum of the synthetic stationary seismic data. After Q filtering, the bandwidth narrows and the dominant frequency decreases (see Figure 6b). The time–frequency spectrum after traditional spectrum-modeling deconvolution is shown in Figure 6c. It can be seen that the bandwidth broadens

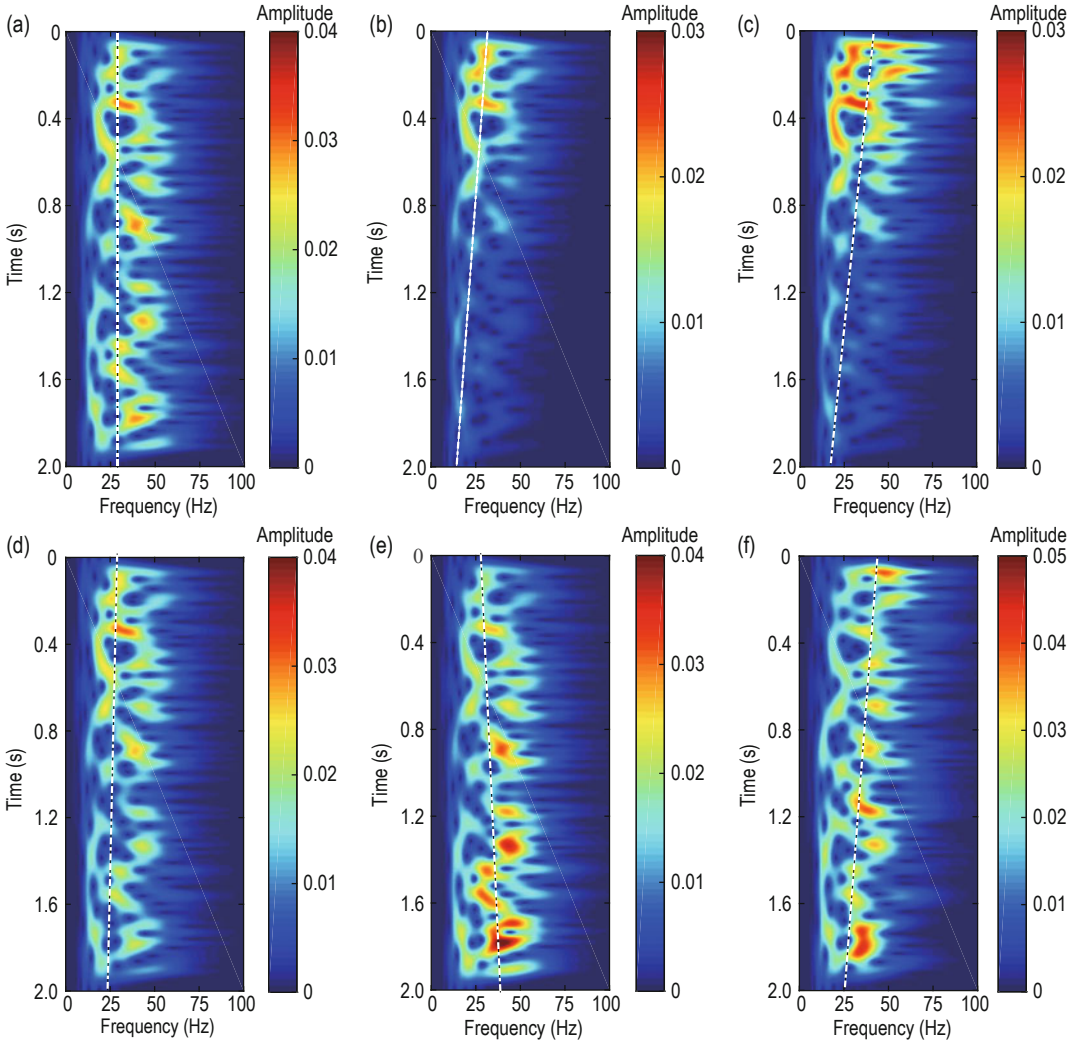

Fig.6 Time–frequency spectrum of Fig. 5 (dashed line is the trend of the dominant frequency change): (a) time–frequency spectrum of Fig. 5a; (b) time–frequency spectrum of Fig. 5b; (c) time–frequency spectrum of Fig. 5c; (d) time–frequency spectrum of Fig. 5d; (e) time–frequency spectrum of Fig. 5e; (f) time–frequency spectrum of Fig. 5f.

and the dominant frequency improves in the shallow layers; however, with increasing time, the seismic data resolution improvement is less clear. Figure 6d shows the time–frequency spectrum for Q compensation with +20% Q estimation error. Because of the +20% overestimation, the deep layers undercompensate. Figure 6e shows the time–frequency spectrum of the Q compensation with −20% Q estimation error. In this case, owing to the underestimation of Q, the deep layers overcompensate. Figure 6f shows the time–frequency spectrum results of the proposed method, the dominant frequency of the shallow, medium, and deep layers has improved, the bandwidth has broadened, the energy of the shallow, medium and deep layers is balanced, and the attenuated energy of the wavelet is reasonably compensated. Based on the data, the frequency band has widened and not is limited by the bandwidth of the source wavelet.

In summary, for nonstationary seismic data, traditional spectrum-modeling deconvolution greatly improves the resolution of the shallow layers but cannot fully compensate for the attenuated wavelet energy; thus, at the middle and deep layers nothing changes. The Q compensation method is affected by the Q estimation. When Q is accurately estimated, it is possible to fully compensate for the attenuation of the seismic wave energy owing to absorption and other factors, and restore the wavelet to the level of the source wavelet. However, the compensation is limited by the bandwidth of the source wavelet. The proposed method can also compensate for the attenuated energy during propagation and the ability to improve the resolution is not limited by the bandwidth of the source wavelet because the bandwidth adapts based on the seismic data.

Field data processing and analysis

To further test the proposed method, we used field seismic records. Figure 7a shows the poststack seismic data of exploration areas, where the resolution gradually decreases with time. Traditional spectrum-modeling deconvolution, Q compensation, and the proposed method are used to improve the resolution of the seismic section and the results are shown in Figures 7b, 7c,

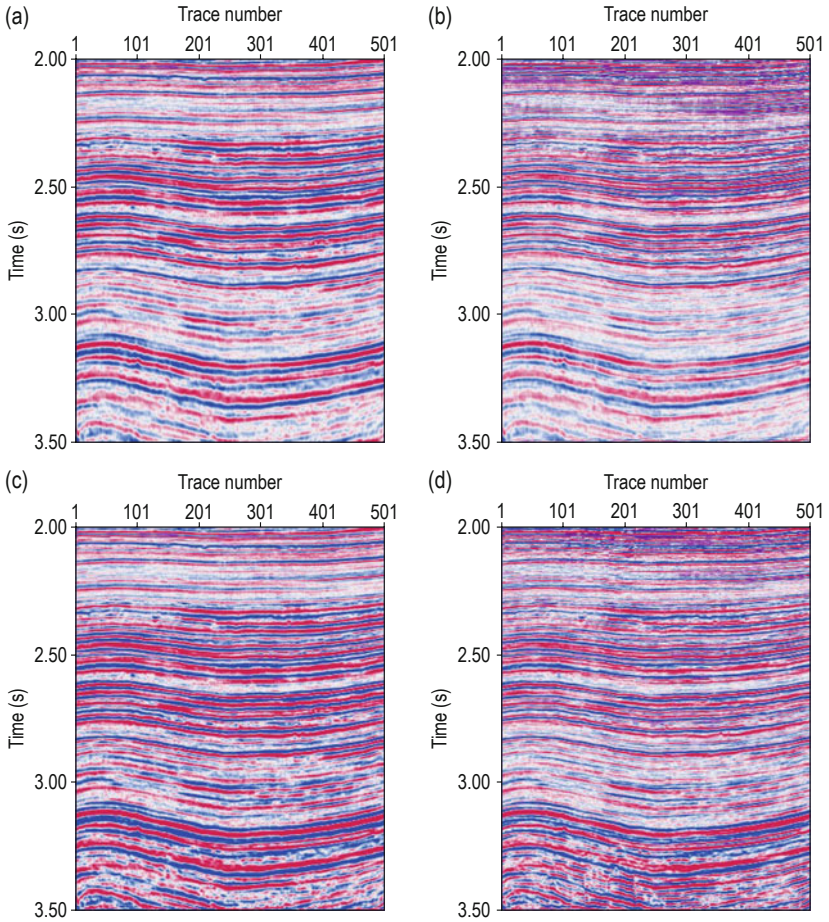

Fig.7 Field data: (a) poststack seismic data; (b) spectrum-modeling deconvolution; (c) Q compensation; (d) proposed method.

and 7d. Clearly, the resolution for shallow and middle formations is improved but not so for the deep layers in Figure 7b. After compensating for energy, the resolution of the middle and deep layers approaches that of the shallow layers in Figure 7c. The improvement, before and after processing with the proposed method, in the resolution of shallow, middle, and deep formations is obvious and the energy of the seismic section is balanced and the continuity of reflections has improved, which helps the interpretation of fine structures.

We also compare the waveform and time–frequency spectrum of traces. The waveform comparison in Figure 8 suggests that the resolution gradually deteriorates with time. The resolution is significantly improved in shallow and middle layers but the amplitude compensation and resolution improvement are not obvious in the deep layers in Figure 8b. The results of the Q compensation method (Figure 8c) clearly show the energy compensation at the middle and deep layers. The resolution after processing with the proposed method (Figure 8d) has obviously improved in shallow and middle layers, and the amplitude is reasonably compensated. Clearly, relative to the Q compensation, the proposed method has improved the resolution in the shallow and middle layers.

Figure 9 shows the time–frequency spectrum of Figure 8. The results after traditional spectrum-modeling deconvolution suggest that the resolution and dominant frequency of the seismic data have improved in the shallow layers; however, there are no changes in the deep layers. The energy compensation and bandwidth broadening of the traditional spectrum-modeling deconvolution mainly affects the shallow and middle layers, whereas the bandwidth in the deep layers is narrow and the high-frequency energy is low. The time

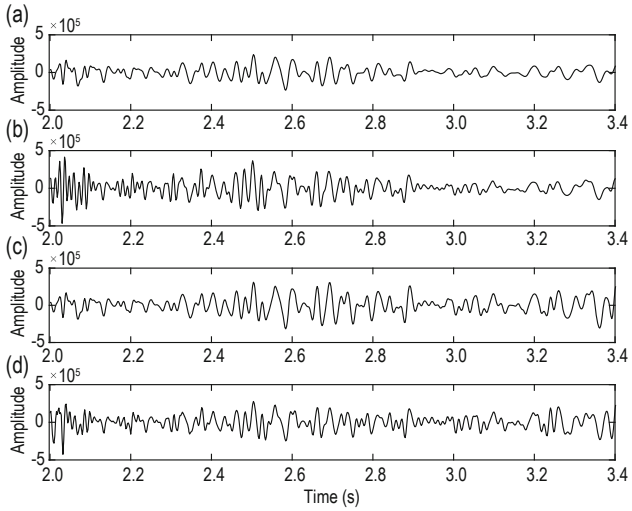

Fig.8 Single trace waveform of Fig. 7: (a) waveform of the 300th trace in Fig. 7a; (b) waveform of the 300th trace in Fig. 7b; (c) waveform of the 300th trace in Fig. 7c; (d) waveform of the 300th trace in Fig. 7d.

–frequency spectrum before and after Q compensation shows that the attenuated energy of the wavelet owing to the absorption by the strata is reasonably compensated and the dominant frequency of the middle and deep layers approaches that of the shallow layers. The proposed method produces frequency bands for each segment that are broad, increases the dominant frequency, and compensates for the energy loss owing to spherical diffusion and absorption by the strata, and balances the reflection energy of the shallow, middle, and deep layers. The proposed method yields dominant frequency and bandwidth that are higher than those of the Q compensation method, without decreasing the SNR.

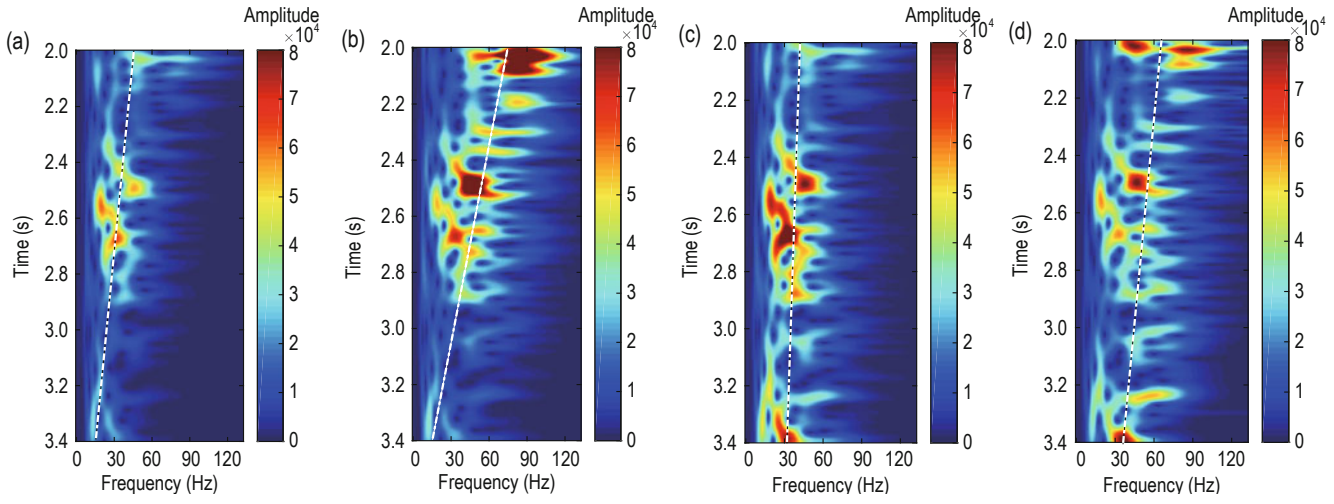

Fig.9 Time–frequency spectrum in Fig. 8: (a) time–frequency spectrum of Fig. 8a; (b) time–frequency spectrum of Fig. 8b; (c) time–frequency spectrum of Fig. 8c; (d) time–frequency spectrum of Fig. 8d.

Conclusions

We propose a seismic resolution enhancement method based on the secondary time–frequency spectrum. Model and field data are used to test this method and the results are compared to those of sepctrum-modeling deconvolution and Q compensation method.

In the secondary time–frequency spectrum, the time-variant wavelet and reflection coefficients are generally separable. The components of the time-variant wavelet are in the center of the spectrum, whereas the main components of the reflection coefficient are adjacent, which facilitates the extraction of the time-variant wavelet.

When nonstationary seismic records are processed, the results of spectrum-modeling deconvolution suggest that the seismic resolution is improved in shallow layers but not in the middle and deep layers. The proposed method does not have these problems and compensates for the energy loss owing to spherical divergence and absorption by strata.

Compared with the Q compensation method, the proposed method does not need to estimate Q and the resolution improvement is not limited by the bandwidth of the source wavelet. Moreover, the method establishes the broadening of the frequency band based on the seismic records.

In principle, the proposed method only considers the amplitude of the wavelet spectrum, which is the same as spectrum whitening, spectrum-modeling deconvolution, and zero-phase filtering, and does not consider the phase of the wavelet. Further processing of the estimates and the elimination of the residual phase of the time-variant wavelet maybe yield better results.

Acknowledgments

We are grateful to the seismic wave propagation and imaging research group at the Department of Geophysics, China University of Petroleum (East China) for help. We would like to thank Prof. Wang Yan-Chun, Prof. Tong Si-You, and Prof. Xu Xiu-Gang for constructive criticism.

References

Ahadi, A., Riahi, M. A., 2013, Application of Gabor deconvolution to zero-offset VSP data: Geophysics, **78**(2), D85−91.

Bai, H., and Li, K. P., 1999, Stratigraphic absorption compensation based on time-frequency analysis: Oil Geophysical Prospecting (in Chinese), **34**(6), 642−648.

Castagna, J. P., Sun, S., and Siegrfied, R. W., 2003, Instantaneous spectral analysis: Detection of low-frequency shadows associated with hydrocarbons: The Leading Eage, **22**(2), 120−127.

Che-Alota, V., Atekwana, E., Atekwana, E., et al., 2008, Geophysical and geochemical attenuated signatures associated with hydrocarbon contaminated site undergoing bioremediation: 78th Ann. Internat. Mtg., Soc. Expl. Geophys., Expanded Abstracts, 2719−2723.

Chen, Z. B., Wang, Y. H., Chen, X. H., et al., 2013, High-resolution seismic processing by Gabor deconvoluton: Journal of Geophysics and Engineering, **10**(6), 065002.

Djeffal, A., Pennington, W., and Askari, R., 2016, Enhancement of Margrave deconvolution of seismic signals in highly attenuating media using the modified S-transform: 86th Ann. Internat. Mtg., Soc. Expl. Geophys., Expanded Abstracts, 5198−5202.

Goloshubin, G. M., and Bakulin, A. V., 1998, Seismic reflectivity of a thin porous fluid-saturated layer versus frequency: 68th Annual Internat. Mtg., Soc, Expl. Geophys., Expanded Abstracts, 976−979.

Goloshubin, G. M., and Korneev, V. A., 2000, Seismic low-frequency effects from fluid saturated reservoir: 70th Ann. Internat. Mtg., Soc. Expl. Geophys., Expanded Abstracts, 1671−1674.

Li, F., Wang, S. D., Chen, X. H., et al., 2013, Prestack nonstationary deconvolution based on variable-step sampling in the radial trace domain: Applied Geophysics, **10**(4), 423−432.

Liu, X. W., Nian J. B., and Liu, H., 2006, Generalized S-transform based compensation for stratigraphic absorption of seismic attenuation: Geophysical Prospecting for Petroleum (in Chinese), **45**(1), 9−14.

Margrave, G. F., and Lamoureux, M. P., 2001, Gabor deconvolution: CREWES Research Report, **13**, 241−276.

Margrave, G. F., Lamoureux, M. P., and Henley, D. C., 2011, Gabor deconvolution: Estimating reflectivity by nonstationary deconvolution of seismic data: Geophysics, **76**(3), W15−W30.

Painter, S., Beresford, G., and Paterson, L., 1995, On the distribution of seismic reflection coefficients and seismic amplitudes: Geophysics, **60**(4), 1187−1194.

Quintal, B., Schmalholz, S. M., and Podladchikov, Y. Y., 2008, Low-frequency reflections from a thin layer with high attenuation caused by interlayer flow: Geophysics, **74**(1), N15−N23.

Ricker, N., 1977, Transient waves in visco-elastic media:

Elsevier Scientific Publishing Company, Amsterdam, 37−67.

Rosa, A. L. R., and Ulrych, T. J., 1991, Processing via spectral modeling: Geophysics, **56**(8), 1244−1251.

Stockwell, R. G., Mansinha, L., and Lowe, R. P., 1996, Localization of the complex spectrum: the S transform: IEEE Transaction on signal processing, **44**(4), 998−1001.

Sun, X. K., Sam, Z. S., and Xie, H. W., 2014, Nonstationary sparsity-constrained seismic deconvolution: Applied Geophysics, **11**(4), 459−467.

Tang, B. W., Zhao, B., Wu, Y. H., et al., 2010, An improved spectral modeling deconvolution: 80th Ann. Internat. Mtg., Soc. Expl. Geophys., Expanded Abstracts, 3668−3672.

Van der Baan, M., 2008, Time-varying wavelet estimation and deconvolution by kurtosis maximization: Geophysics, **72**(2), V11−V18.

Wang, L. L., Gao, J. H., Xu, Z. B., et al., 2014, Hydrocarbon detection using adaptively selected spectrum attenuation: Journal of Applied Geophysics, **105**, 59−66.

Wang, L. L., Gao, J. H., and Zhang, M., 2010, A method for absorption compensation based on adaptive molecular decomposition: Applied Geophysics, **7**(1), 74−87.

Xue, Y. J., Cao, J. X., and Tian, R. F., 2013, A comparative study on hydrocarbon detection using three EMD-based time-frequency analysis methods: Journal of Applied Geophysics, **89**, 108−115.

Zhou, H. L., Wang, J., Wang, M. C., et al., 2014, Amplitude spectrum compensation and phase spectrum correction of seismic data based on the generalized S transform: Applied Geophysics, **11**(4), 468−478.

Wang De-Ying is a Postdoctoral fellow at the Bureau of Geophysical Prospecting, China National Petroleum Corporation. He received his M.S. in Earth Exploration and Information Technology from China University of Petroleum (East China) in 2011. In 2014, he received his Ph.D. in Geological Resources and Geological Engineering from China University of Petroleum (East China). His research interests are seismic data denoizing and resolution enhancement.